

Supporting Information

to

Aggregation controlled photoluminescence hexaazatrinaphthylene (HATN) - experimental and theoretical study

by

Olaf Morawski, Jerzy Karpiuk, Andrzej L. Sobolewski, Paweł Gawryś*

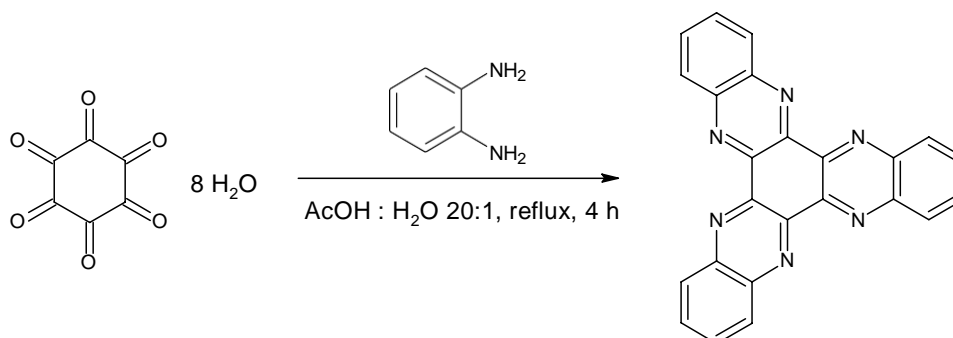
Physics Institute, Polish Academy of Sciences,

Al. Lotników 32/46, Warsaw, Poland

Table of contents

1. Synthesis of 5,6,11,12,17,18-Hexaazatrinaphthylene (HATN).....	2
2. Theoretical results	4
2.1 Results for monomer	4
2.2 Results for dimer	10
3. Experimental results	12
3.1 Optical spectra and emission decays	12
3.2 Transient absorption	15
3.3 Results for crystals	18

1. Synthesis of 5,6,11,12,17,18-Hexaazatrinaphthylene (HATN)



Variant 1. The reaction was carried out without special precautions against oxygen and moisture from air. In a one-necked round-bottom flask (250 ml) equipped with large magnetic stir bar (oval shaped, dimensions at least 5/4 x 5/8 inch) and reflux condenser was put hexaketocyclohexane octahydrate (0.94 g, 3 mmol, Sigma Aldrich), 1,2-diaminobenzene (o-phenylenediamine) (1.08 g, 10 mmol, 3.33 equivalents, Alfa Aesar), acetic acid (at least) (120 ml, POCh-Poland) and water (6 ml). When the reflux temperature was achieved the mixture became dark green and heavy precipitate appeared within a few minutes in the form of fluffy needles. The mixture was vigorously stirred and refluxed for at least 4 hours. Next the temperature of the mantle was cooled to 80°C and after 15 minutes the flask was flooded with methanol as much as possible. The suspension was refluxed for another 30 minutes, cooled slightly and filtered off on a sinter funnel (G2, 3/2 inch diameter) under gentle suction. Next the content of the funnel was washed with methanol (2 x 50 ml). The residue was dried in air for 24 hours and the very dark filtrate was rejected.

The exhausting washing of the green moss-like solid with most organic solvents poorly discolours the green tan from the product. The best results were obtained by stirring the crude product (0.93 g; 80% yield) in the refluxing chloroform (80 ml) in the a one-necked round-bottom flask (250 ml) for at least 6 hours, next to the suspension was added acetone (60 ml) and refluxing was continued overnight (~16h). Next methanol was added (100 ml) and after 6 hours of further boiling the solids were filtered off on a sinter funnel (G2, 3/2 inch diameter) and washed with acetone (2 x 50 ml) and dried in air for 24 hours. Next the solid was collected and dried in vacuum (2 mbar, 60°C) for 8 hours. Yellow solid with greenish tan (0.84 g; 73%).

The solid was suspended in acetic acid (60 ml) and water (50 ml) and under vigorous stirring concentrated nitric acid was added (65%, 10 ml) dropwise. The discoloration of green impurity was fast and after 1 hour the solids were filtered off on a sinter funnel (G2, 3/2 inch diameter) and washed with water (2 x 50 ml) and acetone (2 x 50 ml) and dried shortly. This was followed by stirring of the solids in the mixture acetone (100 ml) and methanol (100 ml) for 24 hours at ambient temperature followed by identical filtration and drying like above. Pale yellow solid.

Variante 2 (recommended, using the ideas from *Chem. Eur. J.* 2007, **13**, 3537 – 3547). The reaction was carried out without special precautions against oxygen and moisture from air. In a two-necked round-bottom flask (250 ml) equipped with large magnetic stir bar (oval shaped, dimensions at least 5/4 x 5/8 inch), optional thermometer and reflux condenser was put hexaketocyclohexane octahydrate (0.94 g, 3 mmol), 1,2-diaminobenzene (o-phenylenediamine) (1.65 g, 15 mmol, 5 equivalents), acetic acid (at least) (120 ml) and water (6 ml). The resultant white suspension was vigorously stirred and heated to reflux with the use of aluminium heating mantle. When the internal temperature exceeded 40°C a pale yellow solution was formed and started to turn green. The solution became dark green when the internal temperature exceeded 60°C and the hexaketone completely dissolved when the internal temperature exceeded 80°C. When the reflux temperature was achieved the mixture became very dark green and heavy precipitate appeared within a few minutes in the form of fluffy needles. The mixture was vigorously stirred and refluxed for at least 4 hours (the temperature of the heating mantle - 130°C and the internal temperature was 115°C). The dark green colour of the suspension gradually faded to pale green-yellow. Next the mixture was cooled so that the internal temperature was 90°C. Water was added through condenser (50 ml) and the heating mantle was taken away. When the internal temperature went below 45°C a mixture of 65% nitric acid and water (1:2 v/v, 60 ml) was added cautiously under vigorous stirring. The mixture changed colour to yellow-orange and the suspension was stirred for additional two hours. Next, the suspension was filtered off on a sinter funnel (slow process, G2, 3/2 inch diameter) and washed with water (2 x 50 ml) and acetone (2 x 50 ml) and dried shortly. The brown colour filtrate was rejected. Next the yellow solid (1.15 g, 100%) was vigorously refluxed for 6 hours in the methanol : water mixture (10:1 v/v, 220 ml) and filtered off again on a sinter funnel (G2, 3/2 inch diameter) and washed with methanol (2 x 50 ml) and dried briefly. This was followed by stirring of the solids in the mixture acetone (100 ml) and methanol (100 ml) for 24 hours at ambient temperature, after which the solids were filtered off on a sinter funnel (G2, 3/2 inch diameter) and washed with acetone (2 x 50 ml) and dried in air for 24 hours. Next the solid was collected and dried in vacuum (2 mbar, 60°C) for 8 hours. Pale yellow solid (1.04 g; 90%).

The product is non-soluble in water and simple alcohols and aliphatic hydrocarbons. It has very poor solubility in all other organic solvents, however the solubility is sufficient for optical measurements. HATN is poorly soluble in chlorinated solvents and only chloroform dissolves it slightly better. Dichloromethane and 1,1,2,2-tetrachloroethane are inferior. Strong acids like trifluoroacetic acid dissolve HATN quite well. The solid does not melt below 360°C.

HATN (50 mg) was casually suspended in chloroform (10 ml) in a sealed vial and left alone. After a less than a week the initially amorphous solid started to convert to transparent glittering blocks and prisms. After two weeks the entire content became crystalline. The crystals were filtered off on a small sinter funnel (G3, 1/2 inch diameter) and washed with chloroform (3 x 10 ml) and dried. The crystals start losing their transparency just after a few minutes. After two hours the crystals became translucent and opaque after a day.

If dichloromethane is used after several weeks very tiny needles and flowers are formed.

2. Theoretical results

2.1 Results for monomer

Table S1. Vertical absorption energy (ΔE), oscillator strength (f), dipole moment (μ), leading electronic configurations and relevant orbitals of the lowest excited states of **hexaazatrinaphthylene** determined with the ADC(2)/cc-pVDZ method at the MP2/cc-pVDZ equilibrium geometry of the ground state. Cartesian components of transition moment and dipole moment are shown.

State	$\Delta E/\text{eV}$	f	μ/Debye	Electronic Configuration
S_0	0.0	-	0.0	$(44a1)^2(7a2)^2(40b1)^2(8b2)^2$
$^3\pi\pi^*$	2.80	-	0.0	$0.64(6a2-9b2)+0.44(7a2-10b2)-0.44(8b2-8a2)$
$^3\pi\pi^*$	2.98	-	1.24	$0.68(7a2-9b2)+0.48(6a2-10b2)$
$^3\pi\pi^*$	2.98	-	-1.24	$0.68(8b2-9b2)-0.48(6a2-8a2)$
$^3n\pi^*$	2.99	-	-0.51	$0.75(40b1-9b2)$
$^3n\pi^*$	2.99	-	0.51	$0.57(40b1-10b2)+0.57(44a1-8a2)+0.44(39b1-9b2)$
$^3n\pi^*$	3.08	-	0.0	$0.75(44a1-9b2)+0.37(43a1-10b2)$
$^1n\pi^*$	3.41	0.0	-0.63(0,0,-0.25)	$0.80(40b1-9b2)$
$^1n\pi^*$	3.41	0.0	0.63(0,0,0.25)	$0.80(44a1-9b2)$
$^1n\pi^*$	3.50	0.0	0.0	$0.75(43a1-9b2)+0.44(44a1-10b2)-0.44(40b1-8a2)$
$^1\pi\pi^*$	3.70	0.0	0.0	$0.65(7a2-8a2)+0.65(8b2-10b2)$
$^1\pi\pi^*$	3.71	0.211(0,0,2.31)	0.97(0,0,0.38)	$0.88(8b2-9b2)$
$^1\pi\pi^*$	3.71	0.211(2.31,0,0)	-0.97(0,0,-0.38)	$0.88(7a2-9b2)$
$^1\pi\pi^*$	3.94	0.0	0.0	$0.74(6a2-9b2)+0.43(7a2-10b2)-0.43(8b2-8a2)$
$^1\pi\pi^*$	4.14	0.057(0,0,0.56)	4.18(0,0,-1.64)	$0.65(6a2-8a2)-0.54(7b2-9b2)$
$^1\pi\pi^*$	4.14	0.057(0.56,0,0)	4.18(0,0,1.64)	$0.65(6a2-10b2)+0.54(5a2-9b2)$
$^1\pi\pi^*$	4.45	0.0	0.0	$0.56(6a2-9b2)-0.55(7a2-10b2)+0.55(8b2-8a2)$
$^1\pi\pi^*$	4.58	1.621(0,0,14.45)	3.76(0,0,1.48)	$0.62(7a2-8a2)-0.65(8b2-10b2)$
$^1\pi\pi^*$	4.58	1.621(14.45,0,0)	-3.76(0,0,-1.48)	$0.62(8b2-8a2)+0.61(7a2-10b2)-0.40(6a2-10b2)$

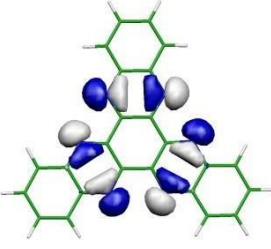
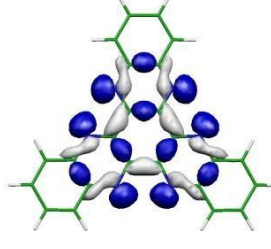
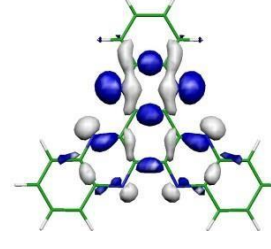
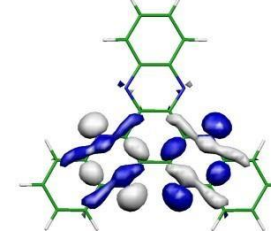
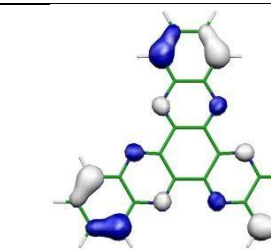
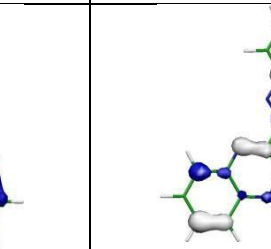
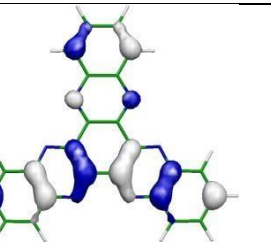
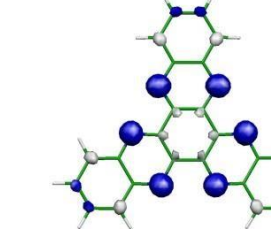
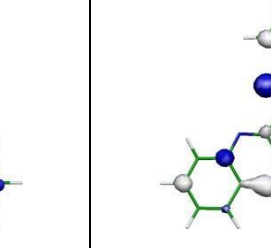
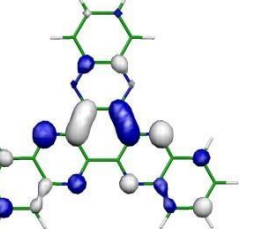
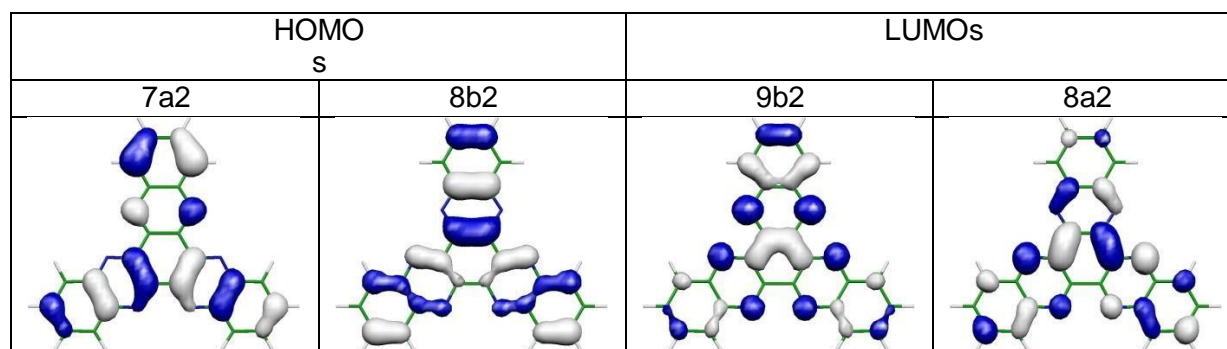
HOMOs			
39b1	43a1	44a1	40b1
			
6a2	8b2	7a2	
			
LUMOs			
9b2	10b2	8a2	
			

Table S2. Vertical emission energy (ΔE), oscillator strength (f), dipole moment (μ), leading electronic configurations, and relevant orbitals of the lowest excited states of **hexaazatrinaphthylene** determined with the ADC(2)/cc-pVDZ method at the equilibrium geometry of a given state. Cartesian components of dipole moments and transition dipole moments are given in parentheses.

singlets

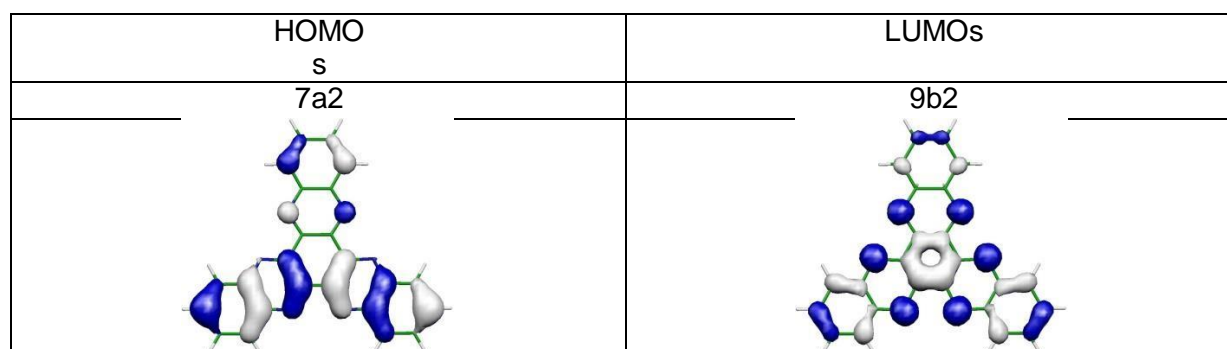
$^1A_1(\pi\pi^*)$

State	$\Delta E/\text{eV}$	f	μ/Debye	Electronic Configuration
S_0	3.43	0.090(0,0,1.07)	0.0(0,0,-0.004)	$(44a1)^2(7a2)^2(40b1)^2(8b2)^2$
$^1\pi\pi^*$	(3.57) _a	-	-0.26(0,0,-0.100)	$0.68(8b2-9b2)+0.48(7a2-8a2)$



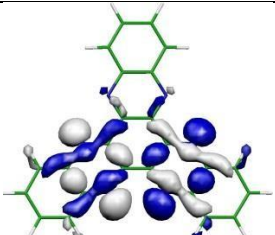
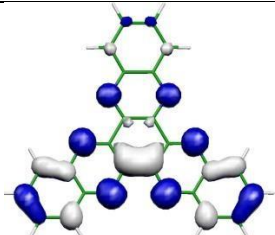
$^1B_1(\pi\pi^*)$

State	$\Delta E/\text{eV}$	f	μ/Debye	Electronic Configuration
S_0	3.50	0.205(2.39,0,0)	0.0(0,0,-0.032)	$(44a1)^2(7a2)^2(40b1)^2(8b2)^2$
$^1\pi\pi^*$	(3.61) _a	-	-1.89(0,0,-0.744)	$0.89(7a2-9b2)$



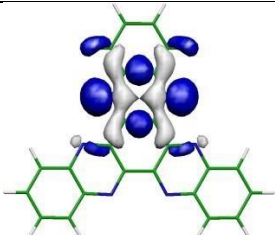
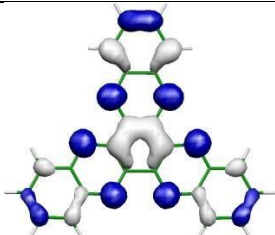
$^1A_2(n\pi^*)$

State	$\Delta E/\text{eV}$	f	μ/Debye	Electronic Configuration
S_0	3.05	0.0	0.05(0,0,-0.020)	$(44a1)^2(7a2)^2(40b1)^2(8b2)^2$
$^1n\pi^*$	(3.25) _a	-	0.05(0,0,0.020)	0.87(40b1-9b2)

HOMO s	LUMOs
40b1	9b2
	

$^1B_2(n\pi^*)$

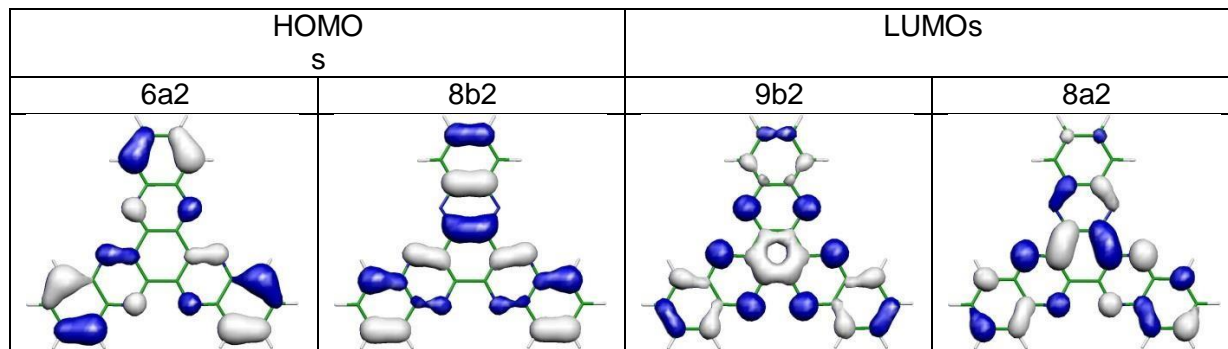
State	$\Delta E/\text{eV}$	f	μ/Debye	Electronic Configuration
S_0	2.75	0.0	0.02(0,0,-0.009)	$(44a1)^2(7a2)^2(40b1)^2(8b2)^2$
$^1n\pi^*$	(3.12) _a	-	0.46(0,0,0.182)	0.84(44a1-9b2)

HOMO s	LUMOs
44a1	9b2
	

a) adiabatic energy

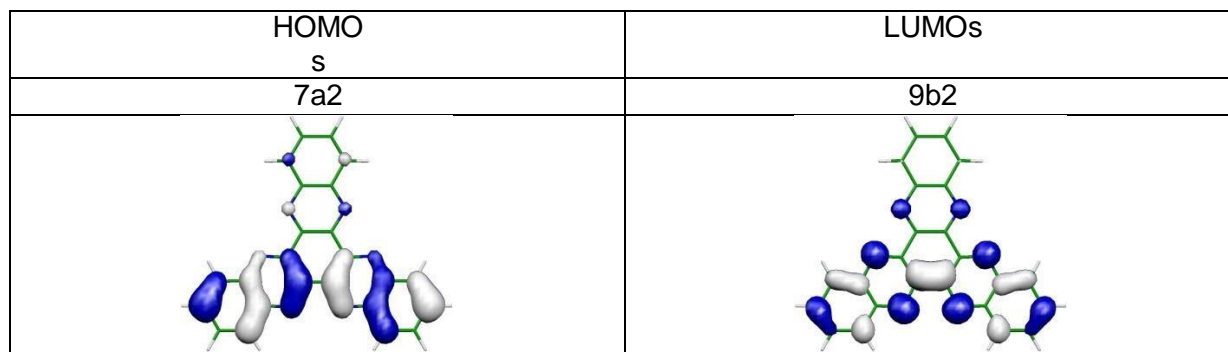
triplets
 $^3A_1(\pi\pi^*)$

State	$\Delta E/eV$	f	μ/Debye	Electronic Configuration
S_0	2.65	-	0.05(0,0,-0.018)	$(44a1)^2(7a2)^2(40b1)^2(8b2)^2$
$^3\pi\pi^*$	(2.81) _a	-	-1.34(0,0,-0.528)	$0.68(8b2-9b2)+0.52(6a2-8a2)$



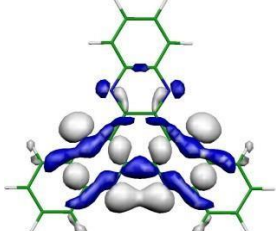
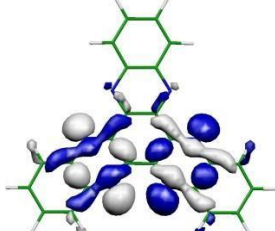
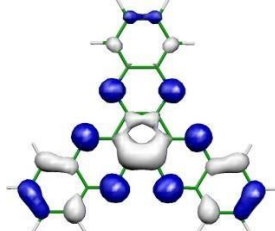
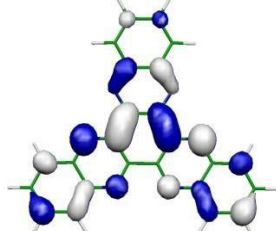
$^3B_1(\pi\pi^*)$

State	$\Delta E/eV$	f	μ/Debye	Electronic Configuration
S_0	2.45	-	0.03(0,0,0.033)	$(44a1)^2(7a2)^2(40b1)^2(8b2)^2$
$^3\pi\pi^*$	(2.66) _a	-	-1.89(0,0,-0.435)	$0.71(7a2-9b2)$



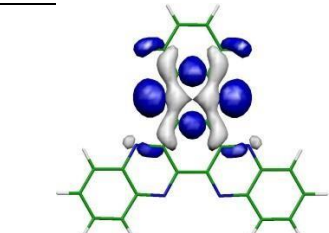
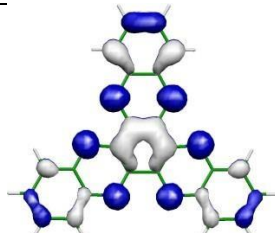
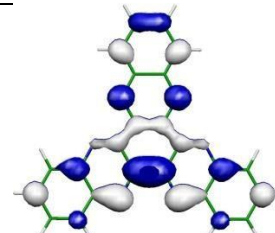
$^3A_2(n\pi^*)$

Stat e	$\Delta E/\text{eV}$	f	μ/Debye	Electronic Configuration
S_0	2.71	0.0	0.06(0,0,-0.023)	$(44a1)^2(7a2)^2(40b1)^2(8b2)^2$
$^3n\pi^*$	(2.86) _a	-	-0.53(0,0,-0.208)	$0.81(40b1-9b2)+0.41(44a1-8a2)$

HOMO s		LUMOs	
44a 1	40b1	9b2	8a2
			

 $^3B_2(n\pi^*)$

Stat e	$\Delta E/\text{eV}$	f	μ/Debye	Electronic Configuration
S_0	2.50	0.0	0.02(0,0,-0.008)	$(44a1)^2(7a2)^2(40b1)^2(8b2)^2$
$^3n\pi^*$	(2.77) _a	-	0.44(0,0,0.173)	$0.80(44a1-9b2)+0.51(44a1-10b2)$

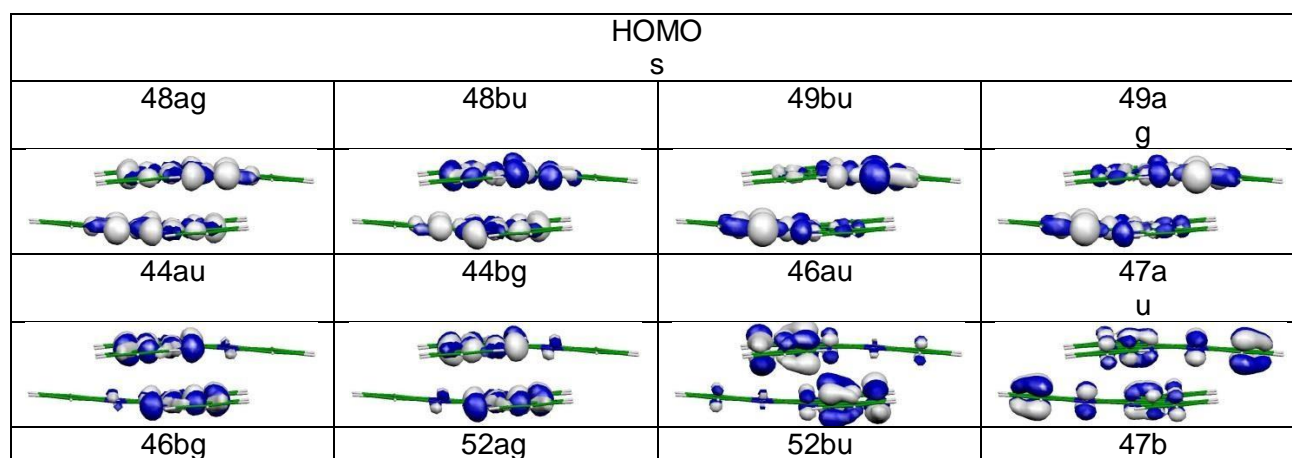
HOMO s	LUMO s	
44a1	9b2	10b2
		

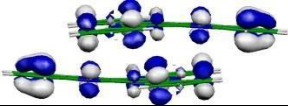
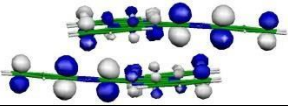
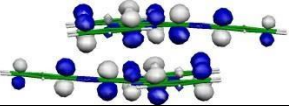
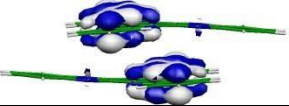
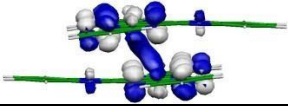
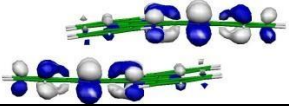
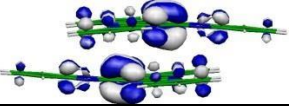
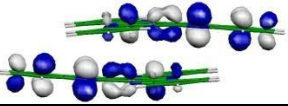
b) adiabatic energy

2.2 Results for dimer

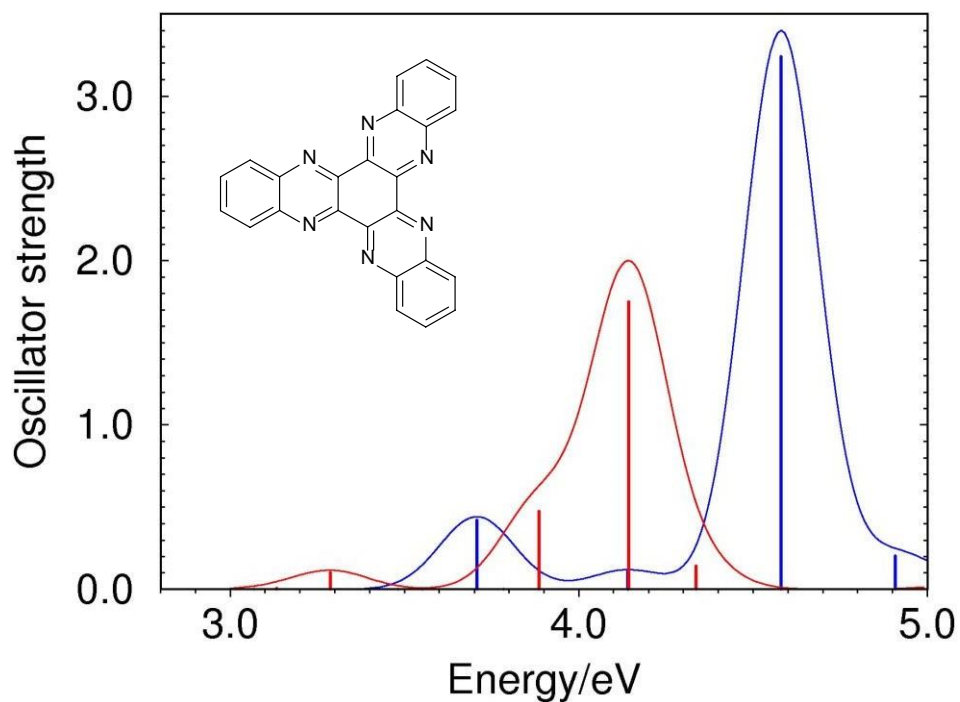
Table S3. Vertical absorption energy (ΔE), oscillator strength (f), dipole moment (μ), leading electronic configurations and relevant orbitals of the lowest excited states of **hexaazatrinaphthylene dimer** determined with the ADC(2)/cc-pVDZ method at the MP2/cc-pVDZ equilibrium geometry of the ground state.

State	$\Delta E/\text{eV}$	f	Electronic Configuration
S_0	0.0	-	$(52ag)^2(47bg)^2(47au)^2(52bu)^2$
${}^3\Pi\Pi^*$	2.67	-	$0.56(47bg-53ag)-0.40(46bg-53ag)$
${}^3\Pi\Pi^*$	2.72	-	$0.45(46bg-53bu)+0.43(46au-53ag)$
${}^3\Pi\Pi^*$	2.84	-	$0.62(52bu-53ag)$
${}^3\Pi\Pi^*$	2.87	-	$0.30(47bg-53bu)-0.33(44au-53ag)$
${}^3\Pi\Pi^*$	2.87	-	$0.53(47au-53bu)+0.40(47bg-53ag)$
${}^3n\Pi^*$	2.89	-	$0.59(44bg-53ag)$
${}^3\Pi\Pi^*$	2.89	-	$0.51(52bu-53bu)+0.40(52ag-53ag)$
${}^3n\Pi^*$	2.90	-	$0.51(44au-53ag)$
${}^3n\Pi^*$	2.91	-	$0.64(49bu-53bu)+0.40(49ag-53ag)$
${}^3n\Pi^*$	2.91	-	$0.64(49ag-53bu)$
${}^3n\Pi^*$	3.00	-	$0.50(48bu-53ag)+0.44(48ag-53bu)$
${}^3n\Pi^*$	3.00	-	$0.45(48bu-53bu)+0.45(48ag-53ag)$
${}^1n\Pi^*$	3.25	0.0	$0.67(44bg-53ag)$
${}^1n\Pi^*$	3.25	0.004	$0.64(44au-53ag)+0.42(44bg-53bu)$
${}^1n\Pi^*$	3.28	0.0	$0.68(49ag-53bu)+0.44(49bu-53ag)$
${}^1n\Pi^*$	3.28	0.0	$0.68(49bu-53bu)+0.45(49ag-53ag)$
${}^1\Pi\Pi^*$	3.34	0.049	$0.85(47bg-53bu)$
${}^1\Pi\Pi^*$	3.37	0.021	$0.52(48bu-53ag)+0.42(48ag-53bu)$
${}^1\Pi\Pi^*$	3.36	0.0	$0.85(47bg-53ag)$
${}^1\Pi\Pi^*$	3.40	0.034	$0.76(52bu-54ag)$
${}^1\Pi\Pi^*$	3.40	0.0	$0.61(47bg-48bg)$
${}^1\Pi\Pi^*$	3.54	0.085	$0.56(52ag-53bu)+0.42(52bu-54ag)$



			
LUMO s			
53ag	53bu	48bg	54a g
			

(a)



(b)

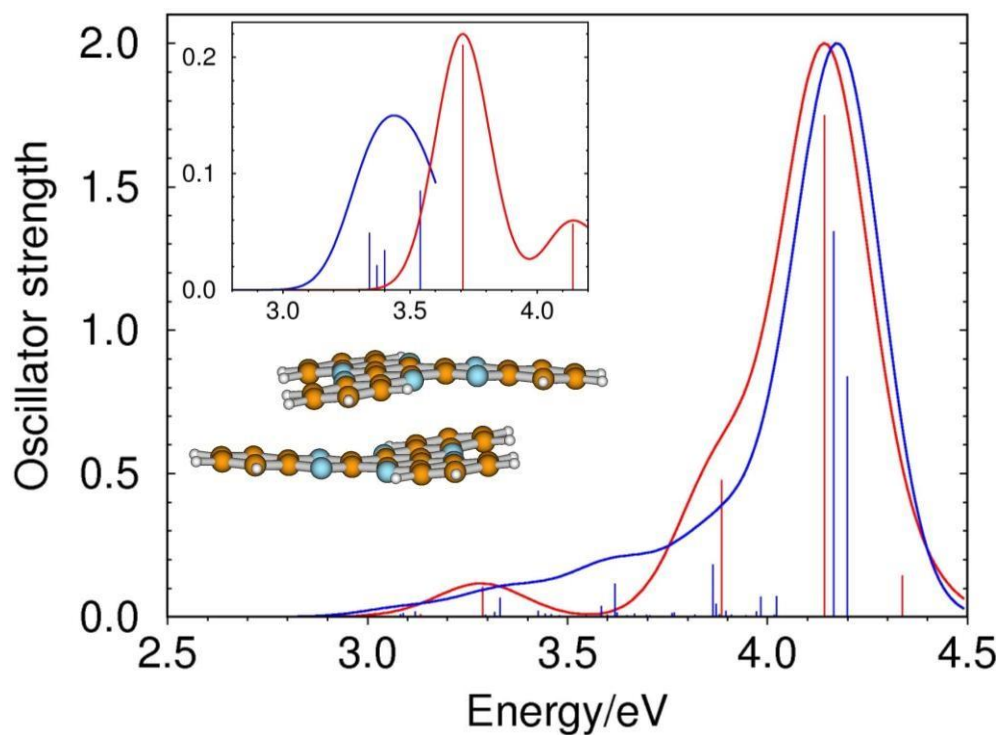


Figure S1. Absorption spectrum of HATN: (a) monomer computed with the ADC(2)/cc-pVDZ method (blue) and with the TDDFT/B3-LYP/cc-pVDZ method (red), (b) monomer (red) and dimer (blue) computed with the TDDFT/B3-LYP/cc-pVDZ method. Insert shows the red part of the respective spectra computed with the ADC(2)/cc-pVDZ method. The computed stick spectra were convoluted with Gaussian function of 0.25 eV FWHM.

3. Experimental results

3.1 Optical spectra and emission decays

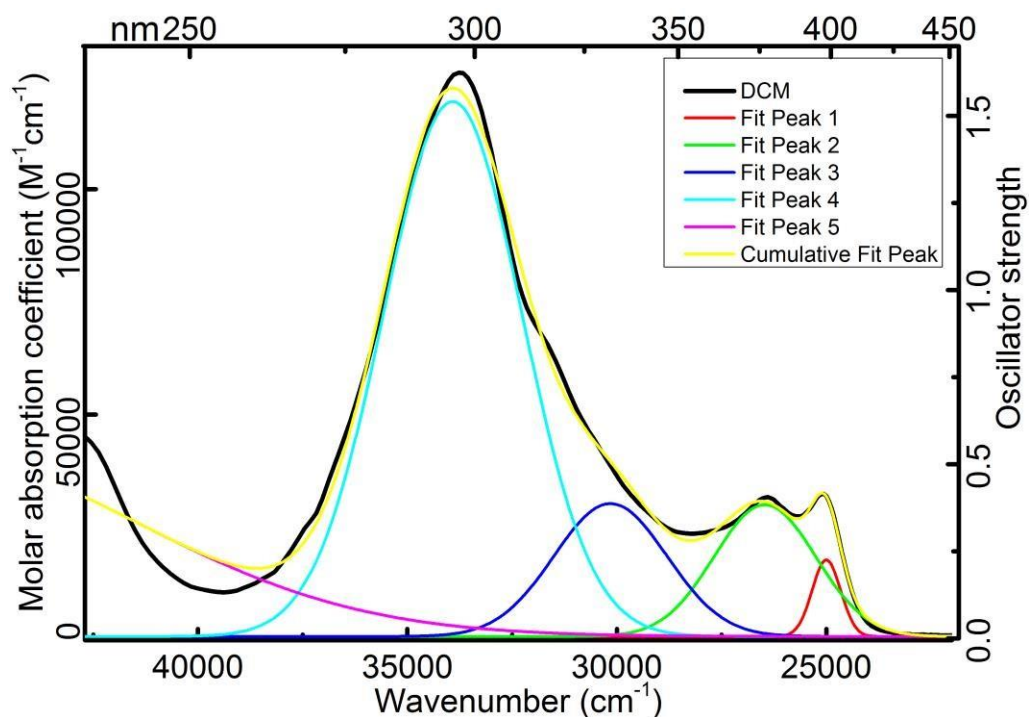


Figure S2. Fit of five Gaussian bands to absorption spectrum of HATN in DCM.

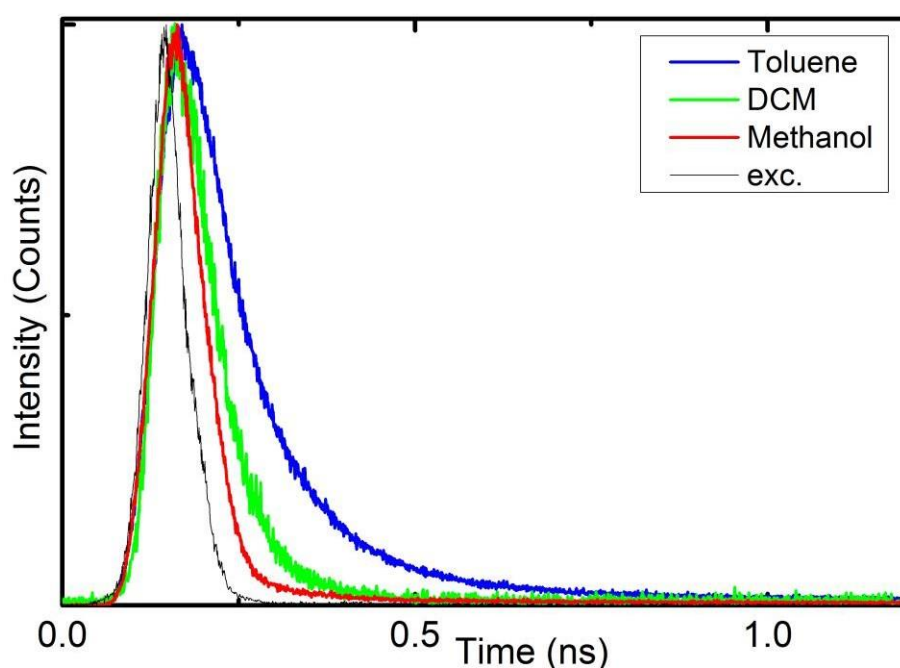


Figure S3. Normalised fluorescence decays of HATN in solvents at room temperature observed at 440 nm (colour lines) and excitation pulse (black line). Temporal resolution 0.814 ps per channel. Excitation at 390 nm.

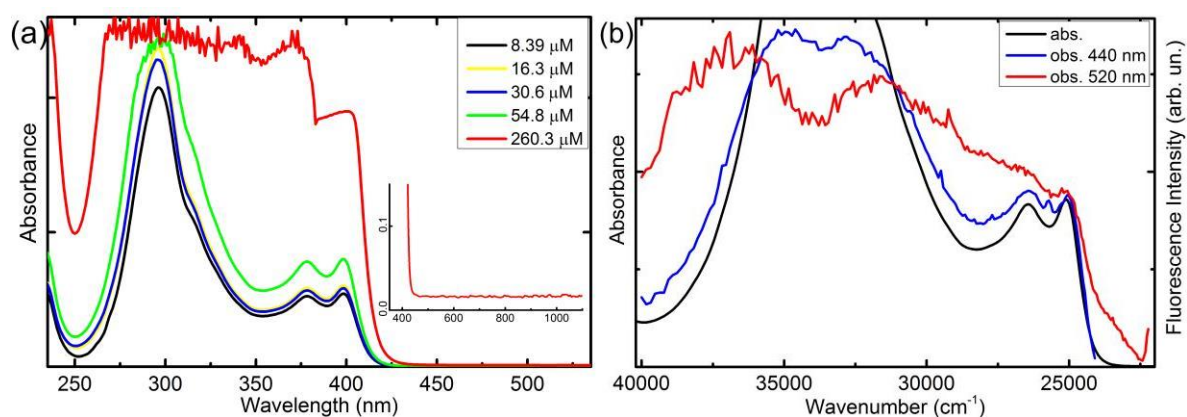


Figure S4. Shape of absorption spectrum of HATN in DCM at several concentrations at 20⁰ C (a) and fluorescence excitation spectrum at 46 μM (b). To ease the comparison in (a) absorption spectra are recalculated to similar height, in (b) fluorescence excitation spectra and absorption spectrum are normalised at 399 nm. Inset to (a) presents absorption spectrum at long wavelengths recorded for concentration 260 μM. Flat line suggests no J-aggregates are formed at this high concentration, but cannot exclude H-aggregates.

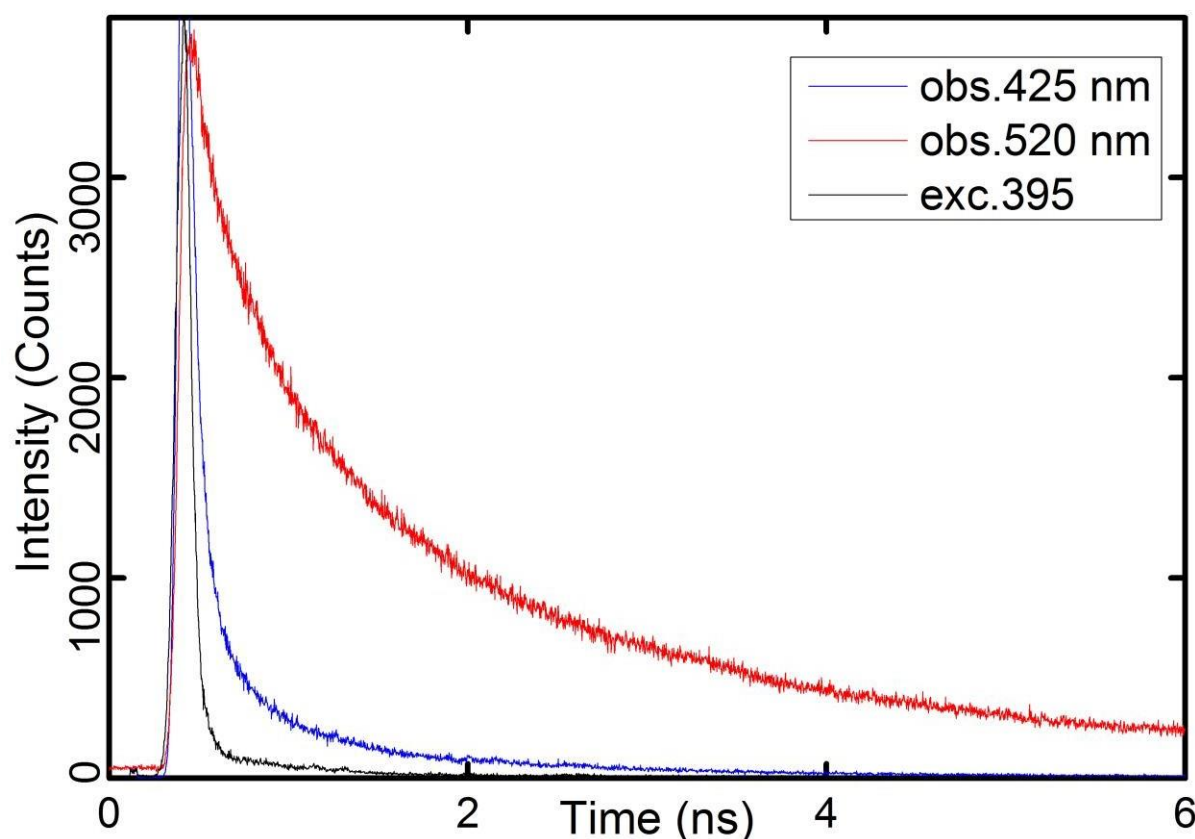


Figure S5. Plot of normalised fluorescence decays of 46 μM HATN in DCM at room temperature observed at 425 and 520 nm (blue and red lines) and excitation pulse (black line). Temporal resolution 2.44 ps per channel. Excitation at 395.5 nm.

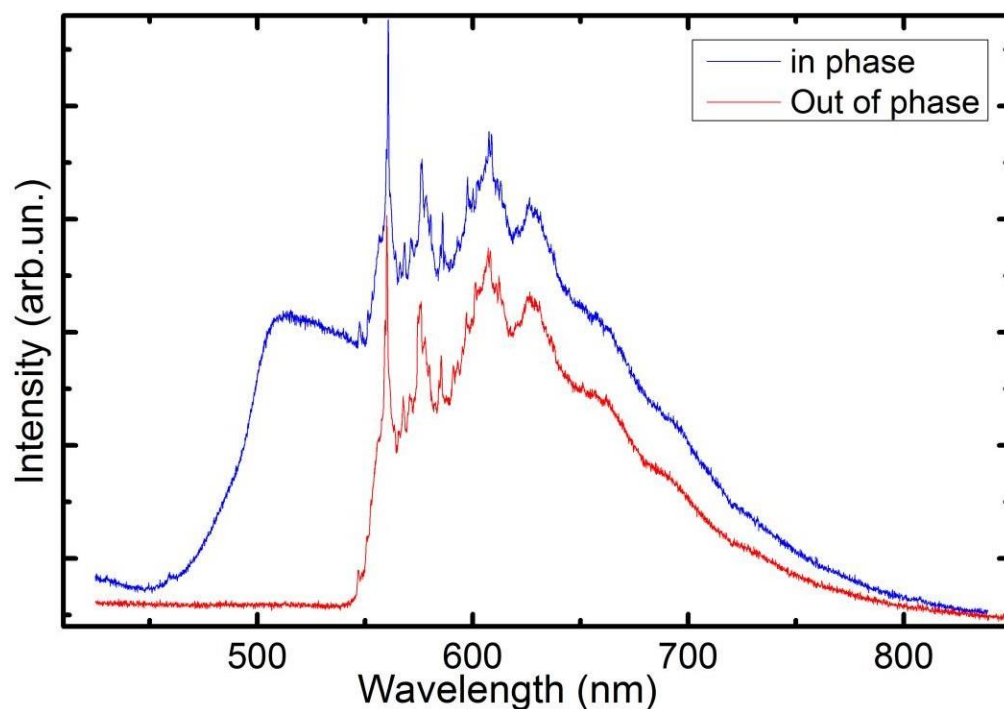


Figure S6. Emission spectra of HATN in DCM recorded at temperature 5 K with phosphoroscope of factor $f_{\text{phs}}=3$. The “In phase” spectrum (blue line) taken with excitation and observation choppers working in-phase contains fluorescence and phosphorescence photons, the “Out of phase” spectrum comprises of phosphorescence only as the out-of-phase observation chopper blocks the short lived fluorescence. Excitation at 405 nm.

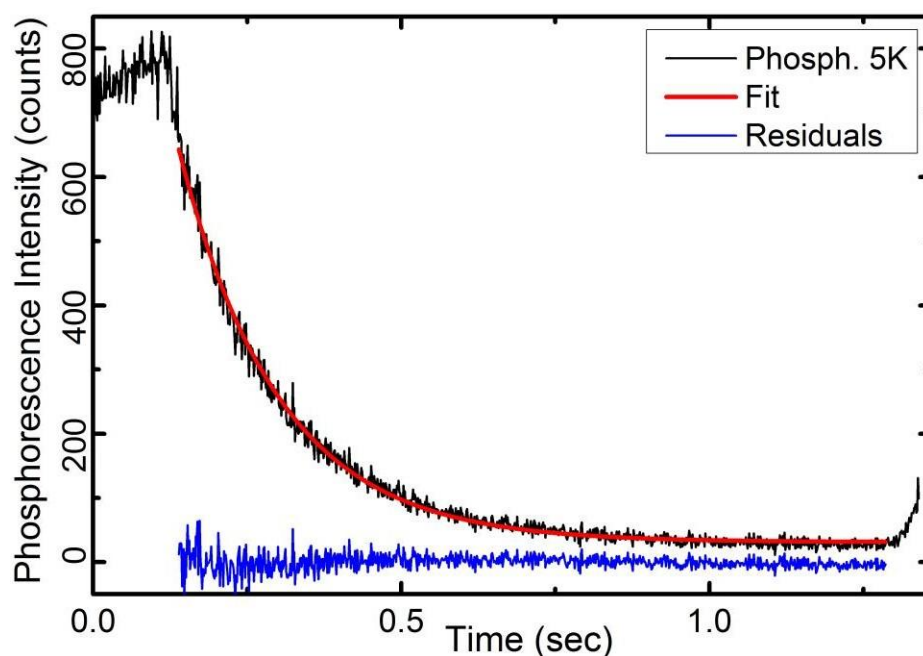
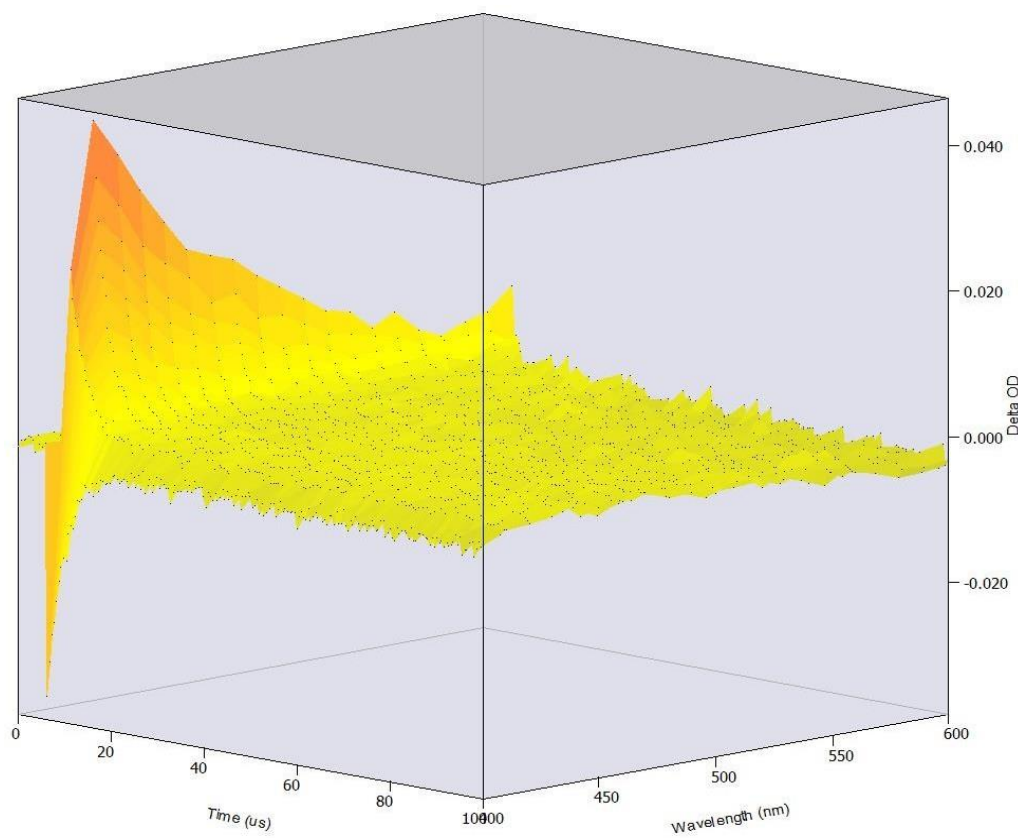
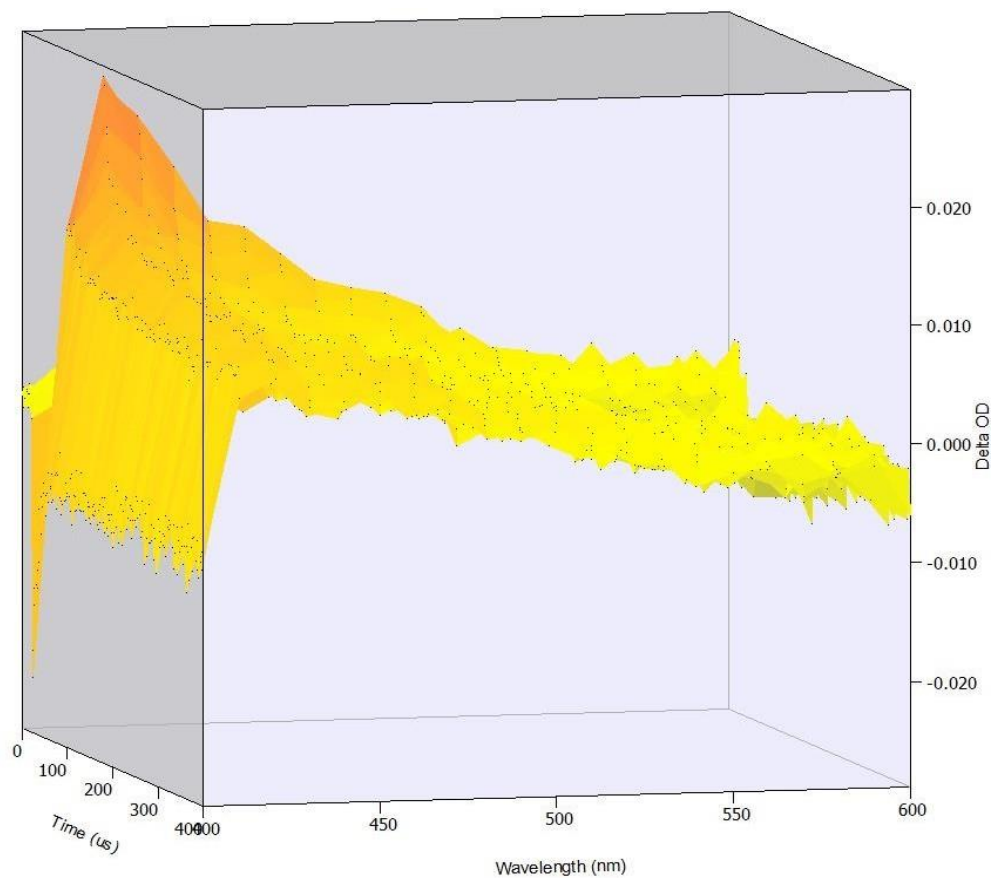


Figure S7. Phosphorescence decay of HATN in DCM observed at 560 nm and recorded at temperature 5 K (black line). The exponential fit (red line) and fitting residuals (blue line) are also presented. The calculated phosphorescence decay time is 164 ± 1 ms. Excitation at 405 nm. Temporal resolution 1.31 ms per channel.

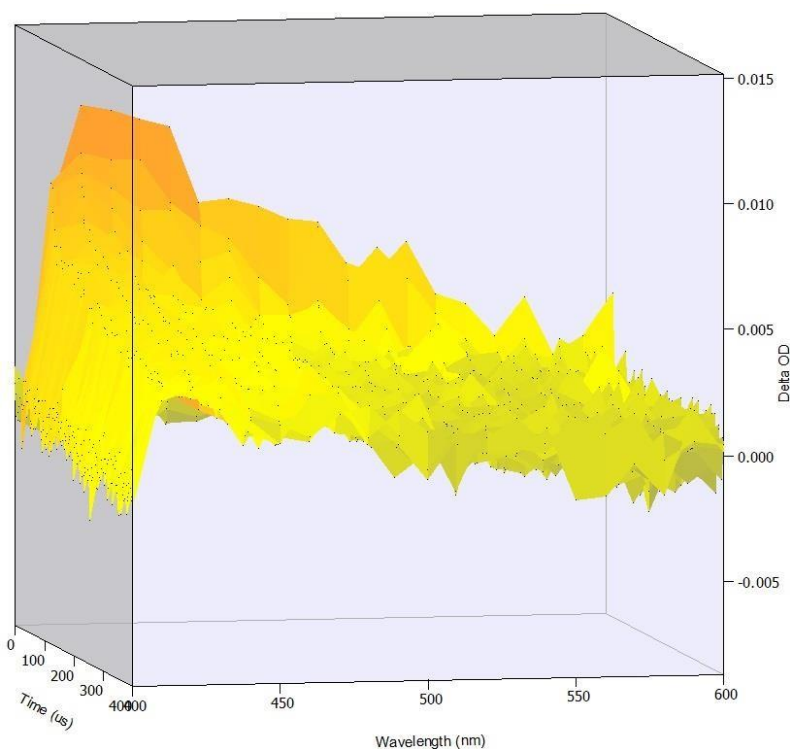
3.2 Transient absorption



(a)



(b)



(c)

Figure S8. Three-dimensional transient absorption spectrum of diluted HATN solutions after irradiation by a 310 nm laser pulse. Solvents: (a) dichloromethane, (b) methanol, (c) toluene. In dichloromethane the spectrum decays mono-exponentially at all wavelengths, in methanol and toluene a second decay component is observed at 410 – 520 nm. The negative absorption for short times at 400 nm, the region of stationary absorption onset, is assigned to a ground state bleaching.

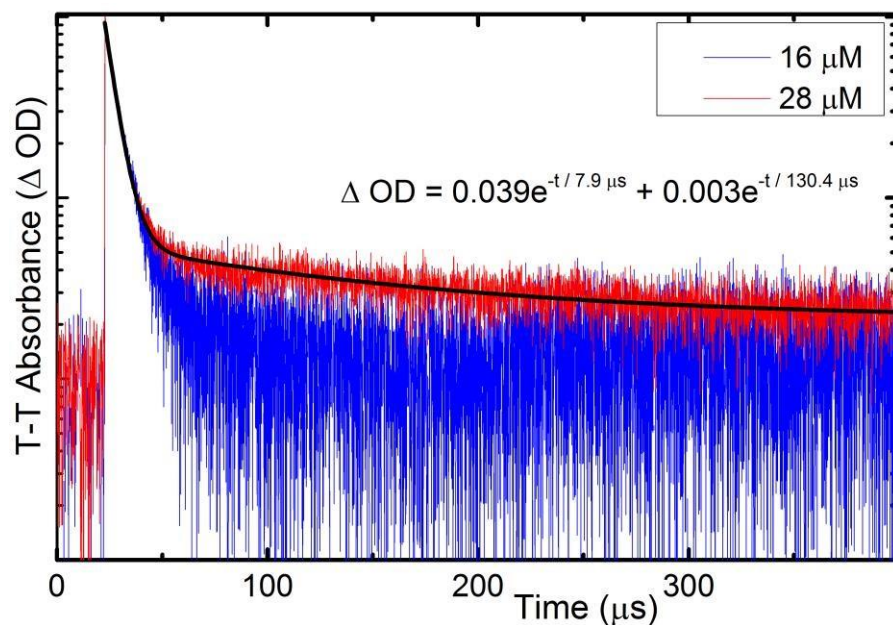


Figure S9. HATN in DCM, semi-logarithmic plot of normalized decay profiles of transient absorption observed at 420 nm after excitation with a 310 nm laser pulse. Black line represents two exponential fit to 28 μM trace. Legend specifies concentrations of the solute.

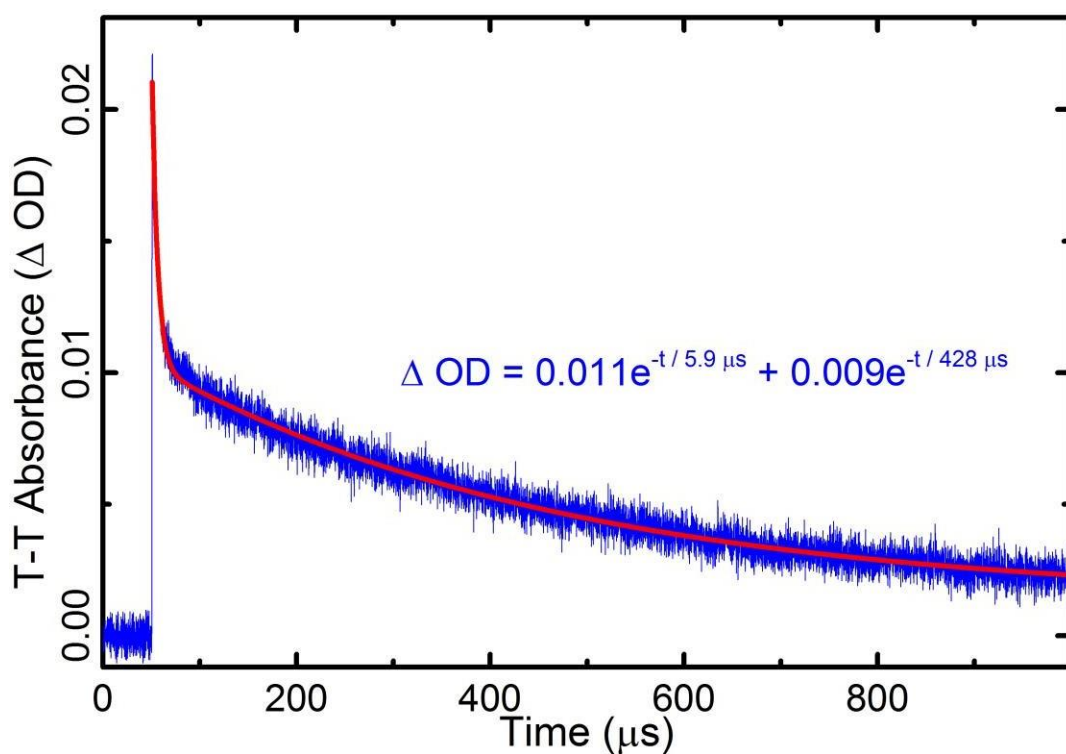


Figure S10. HATN in toluene, the decay profile of transient absorption spectrum observed at 420 nm after excitation with a 310 nm laser pulse. Red line represents two exponential fit to experimental data with decay times: $\tau_1 = 5.9 \pm 0.1 \mu s$ and $\tau_2 = 428 \pm 4 \mu s$.

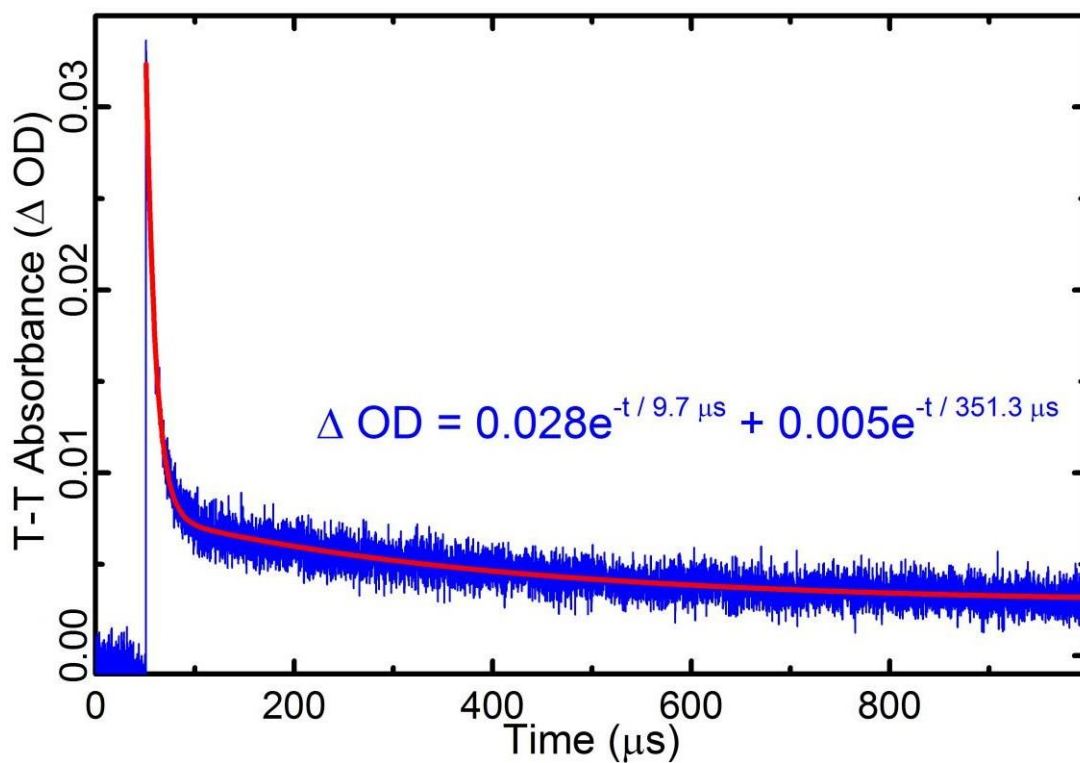
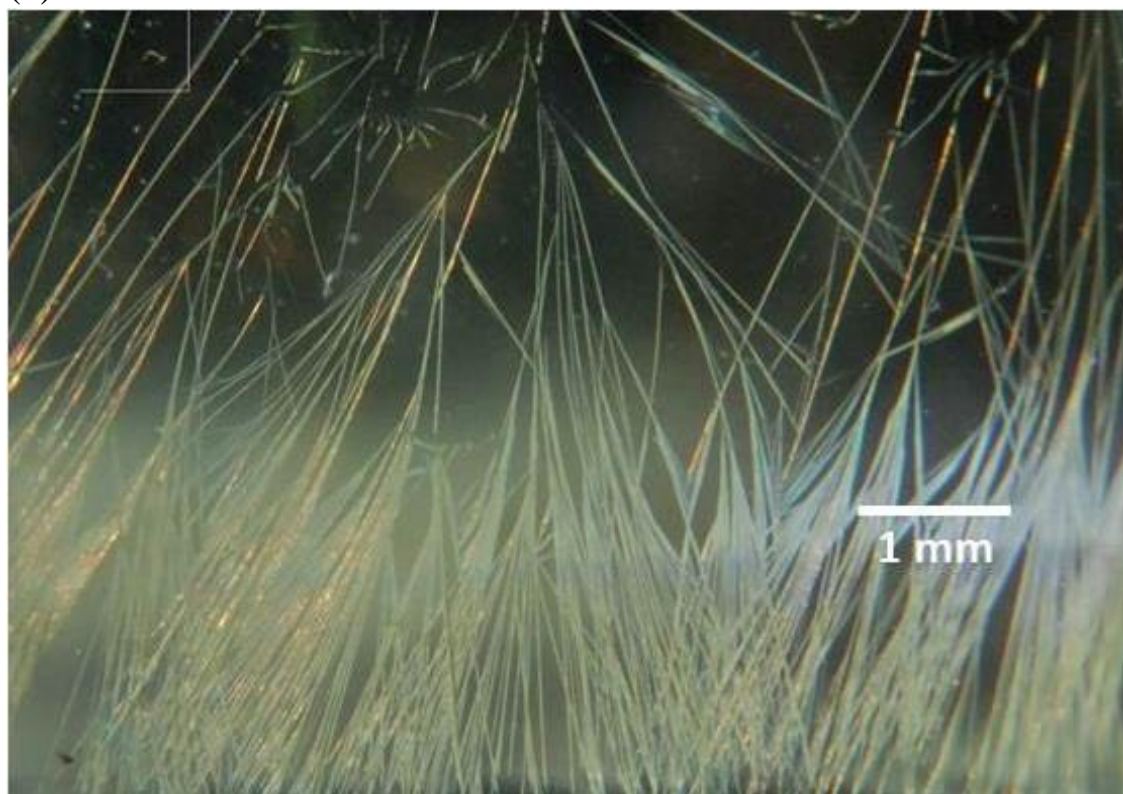


Figure S11. HATN in methanol, the decay profile of transient absorption spectrum observed at 420 nm after excitation with a 310 nm laser pulse. Red line represents two exponential fit to experimental data with decay times: $\tau_1 = 9.7 \pm 0.1 \mu s$ and $\tau_2 = 351 \pm 8 \mu s$.

3.3 Results for crystals

(a)



(b)

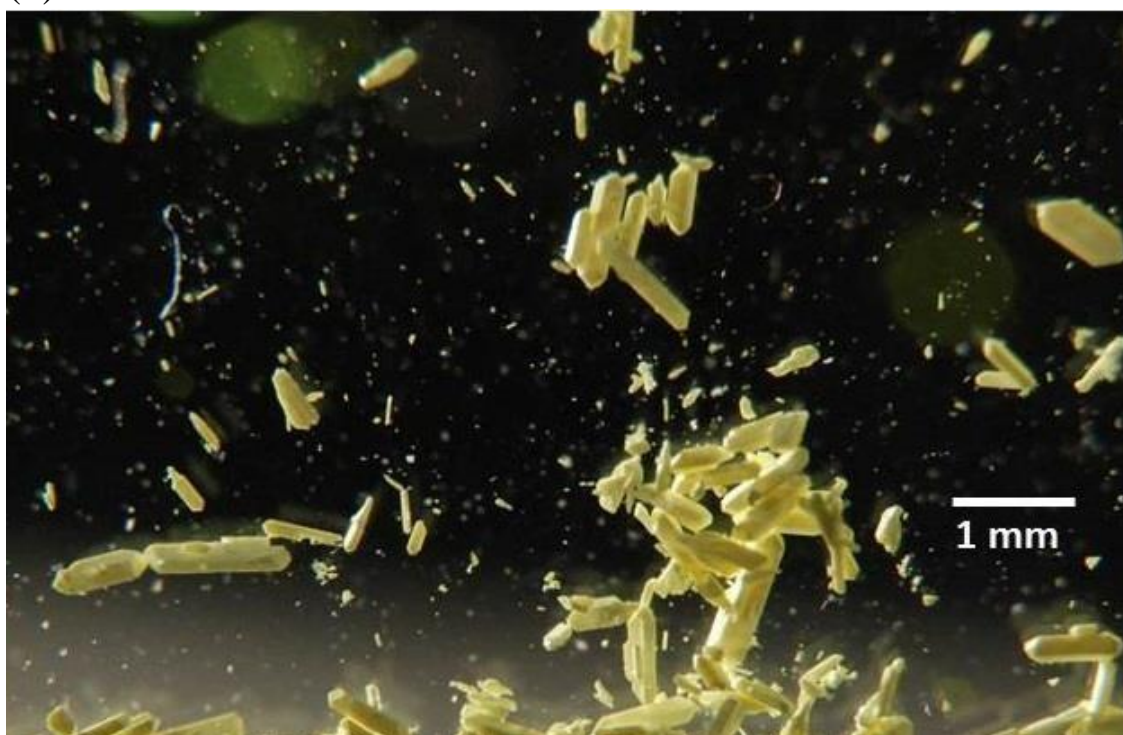


Figure S12. Crystals of HATN: (a) needles grown from dichloromethane and (b) rectangular prisms grown from chloroform.

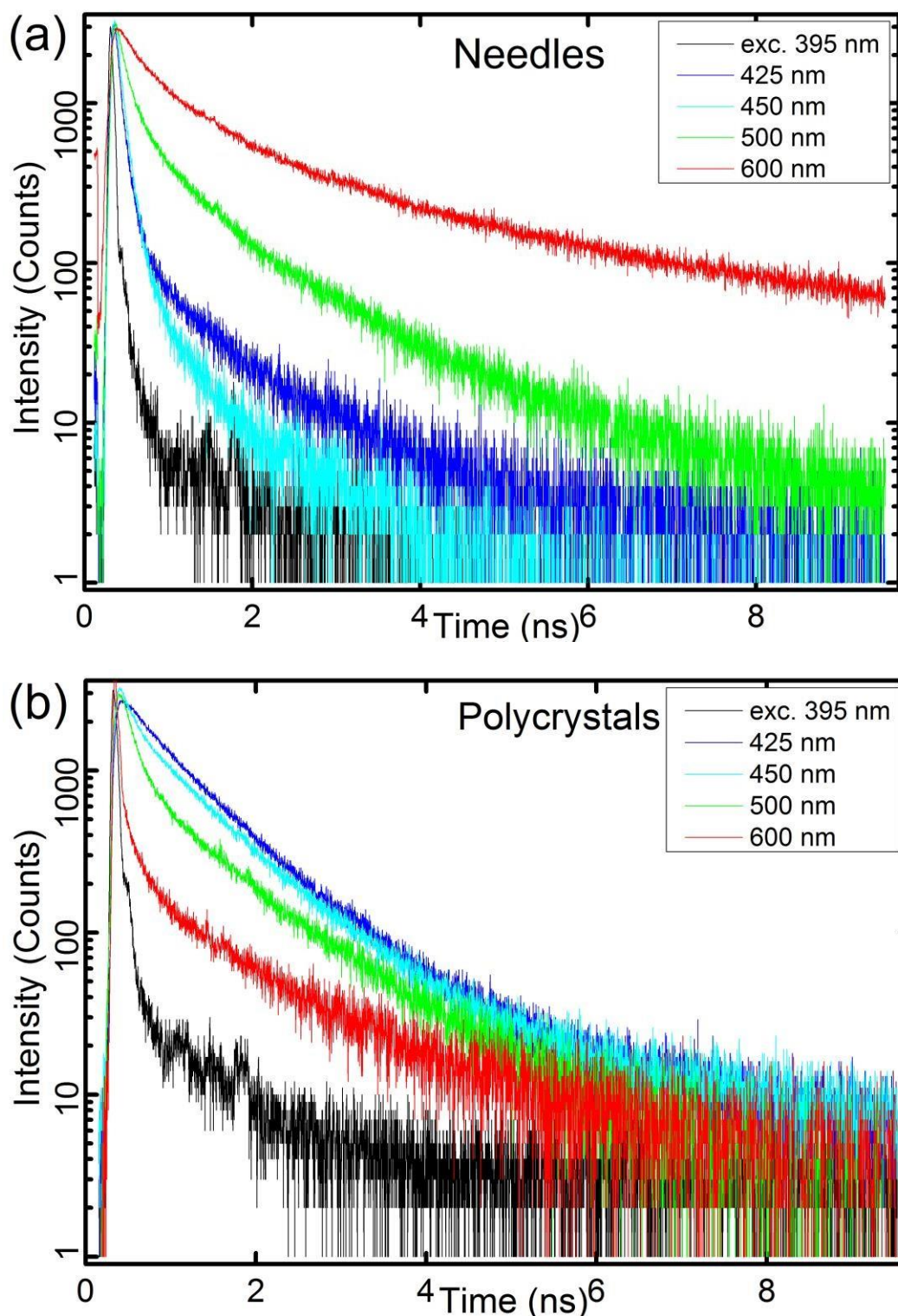


Figure S13. Semilogarithmic plots of fluorescence of HATN crystals: (a) needles grown from dichloromethane and (b) rectangular prisms grown from chloroform. Temporal resolution 2.44 ps per channel. Excitation at 395.5 nm. Legend specifies colours of decay traces and wavelength of observation.